THEMIS observation of chorus elements without a gap at half the gyrofrequency

AUTHOR(S):

Kurita, S.; Katoh, Y.; Omura, Y.; Angelopoulos, V.; Cully, C. M.; Le Contel, O.; Misawa, H.

CITATION:

Kurita, S. ...[et al]. THEMIS observation of chorus elements without a gap at half the gyrofrequency. Journal of Geophysical Research: Space Physics 2012, 117(A11): A11223.

ISSUE DATE:

2012-11

URL:

http://hdl.handle.net/2433/193717

JOURNAL OF GEOPHYSICAL RESEARCH, VOL. 117, A11223, doi:10.1029/2012JA018076, 2012

THEMIS observation of chorus elements without a gap at half the gyrofrequency

S. Kurita,[1] Y. Katoh,[2] Y. Omura,[3] V. Angelopoulos,[4] C. M. Cully,[5,6] O. Le Contel,[7] and H. Misawa[1]

Received 28 June 2012; revised 8 September 2012; accepted 11 October 2012; published 30 November 2012.

[1] Using waveform data obtained by one of the THEMIS satellites, we report properties of rising tone chorus elements without a gap at half the gyrofrequency in a region close to the magnetic equator. The wave normal angle of the chorus elements is typically field-aligned in the entire frequency range of both upper-band and lower-band chorus emissions. We find that the observed frequency sweep rates are consistent with the estimation based on the nonlinear wave growth theory of Omura et al. (2008). In addition, we compare the frequency profiles of the chorus wave amplitudes with those of the optimum and threshold wave amplitudes derived from the nonlinear wave growth theory for triggering rising tone chorus emissions. The results of the comparison show a reasonable agreement, indicating that rising tone chorus elements are continually generated through a triggering process which generates elements with the optimum amplitudes for nonlinear growth.

Citation: Kurita, S., Y. Katoh, Y. Omura, V. Angelopoulos, C. M. Cully, O. Le Contel, and H. Misawa (2012), THEMIS observation of chorus elements without a gap at half the gyrofrequency, *J. Geophys. Res.*, *117*, A11223, doi:10.1029/2012JA018076.

1. Introduction

[2] In the Earth's inner magnetosphere, whistler mode chorus emissions are observed mostly on the dawn and day side and are enhanced during geomagnetically disturbed periods [*Tsurutani and Smith*, 1974; *Meredith et al.*, 2001]. Chorus emissions are narrow band emissions observed in the typical frequency range of 0.2 to 0.8 Ω_{e0} with a gap at 0.5 Ω_{e0}, where Ω_{e0} is the electron gyrofrequency Ω_e at the magnetic equator. Emissions below and above 0.5 Ω_{e0} are called the lower-band and upper-band chorus emissions, respectively. Based on the duct propagation characteristics of whistler mode waves, *Bell et al.* [2009] showed that the gap at 0.5 Ω_{e0} can be formed if the lower- and upper-band chorus waves are generated within the enhanced and depleted plasma density region, respectively. Results of in situ observation [*Santolík et al.*, 2003; *Li et al.*, 2011] revealed that the wave normal angles of the lower-band chorus emissions are typically field-aligned in the equatorial region and become large on the dayside of the region away from the equator. On the other hand, upper-band chorus emissions have weaker wave magnetic amplitude and larger wave normal angle compared with the lower-band chorus emissions, and are observed in a confined region close to the magnetic equator [*Li et al.*, 2011]. Because of the difference, the generation processes of the upper-band and lower-band chorus emissions have sometimes been discussed separately.

[3] As the generation mechanism of chorus, effects of nonlinear wave-particle interactions have been discussed by considering a coherent wave element propagating along the magnetic field line [*Omura et al.*, 1991]. Recently, *Omura et al.* [2008] have proposed a nonlinear wave growth theory for the generation process of rising tone chorus emissions. Based on the theory, a frequency sweep rate of a rising tone chorus element depends on the wave amplitude of an individual wave packet. On the other hand, *Trakhtengerts* [1995] and *Trakhtengerts et al.* [2004] proposed the Backward Wave Oscillator (BWO) model as a generation model of chorus emissions. BWO model proposed that frequency sweep rates depend on background plasma parameters such as plasma density and magnetic field strength. The validity of the relationship proposed by *Omura et al.* [2008] was confirmed by comparing with simulation results [*Hikishima et al.*, 2009; *Katoh and Omura*, 2011] and was also demonstrated by observation [*Cully et al.*, 2011]. The dependence of the frequency sweep rate predicted by BWO model was compared

[1]Planetary Plasma and Atmospheric Research Center, Graduate School of Science, Tohoku University, Sendai, Japan.
[2]Department of Geophysics, Graduate School of Science, Tohoku University, Sendai, Japan.
[3]Research Institute for Sustainable Humanosphere, Kyoto University, Uji, Japan.
[4]Institute of Geophysics and Planetary Physics, University of California, Los Angeles, California, USA.
[5]Swedish Institute of Space Physics, Uppsala, Sweden.
[6]Now at Department of Physics and Astronomy, University of Calgary, Calgary, Alberta, Canada.
[7]Laboratoire de Physique des Plasmas, CNRS/Ecole Polytechnique/UPMC/Paris-Sud 11, St. Maur-des-Fossés, France.

Corresponding author: S. Kurita, Planetary Plasma and Atmospheric Research Center, Graduate School of Science, Tohoku University, Sendai, Miyagi 980-8578, Japan. (kurita@pparc.gp.tohoku.ac.jp)

0148-0227/12/2012JA018076

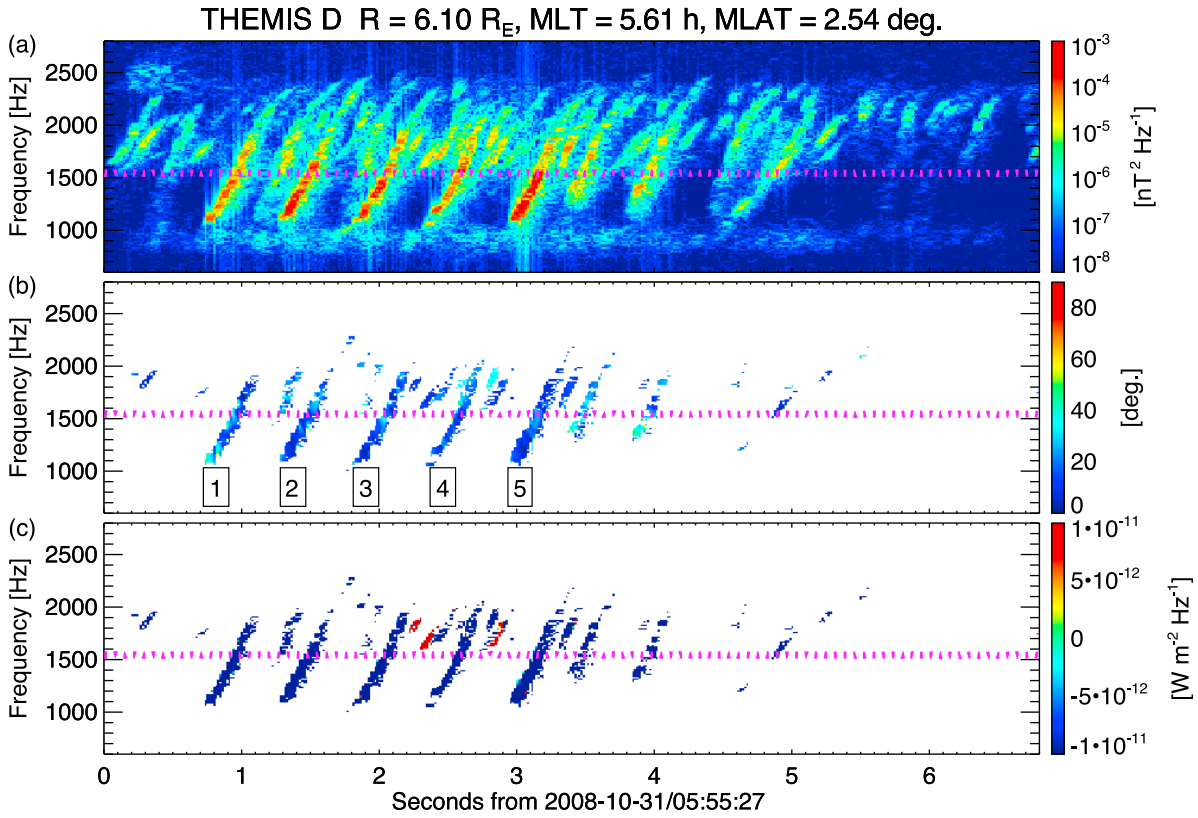

Figure 1. Chorus emissions without a distinct gap at half the electron gyrofrequency observed from 05:55:27 to 05:55:33.8 UT on 31 October 2008 by THEMIS D. (a) Wave spectral intensity in magnetic field. (b) Wave normal angle and (c) the Poynting vector parallel to the ambient magnetic field, respectively. The results of Figures 1b and 1c are shown only when the magnetic wave spectral intensity is greater than 10^{-5} nT^2/Hz. The dotted lines in Figures 1b and 1c represent half the local gyrofrequency estimated from FGM.

with the observations by Cluster [*Macúšová et al.*, 2010] and THEMIS [*Tao et al.*, 2012].

[4] *Omura et al.* [2009] have suggested that a rising tone chorus element is generated in the region close to the magnetic equator through the nonlinear wave growth mechanism in the purely field aligned direction, and that the gap at 0.5 Ω_{e0} is formed by a nonlinear wave damping during its propagation away from the equator with a slightly oblique wave normal angle, resulting in the separation of chorus emissions into the upper-band and lower-band chorus emissions. Chorus emissions without a gap at 0.5 Ω_{e0} are expected to be observed in the source region based on the nonlinear wave growth/damping mechanisms. *Burtis and Helliwell* [1976] have reported the presence of the chorus emissions without a gap at 0.5 Ω_{e0} in the region close to the magnetic equator based on the OGO-3 observations. It is interesting to analyze the properties of the chorus emissions without a gap at 0.5 Ω_{e0} whether the observed properties are consistent with the theoretical predictions by the nonlinear wave growth theory or not.

[5] In the present study we analyzed the properties of rising tone chorus elements without a gap at half the gyrofrequency observed by the THEMIS spacecraft in the region close to the magnetic equator. The frequency sweep rates of the chorus emissions were compared with the prediction by the nonlinear wave growth theory [*Omura et al.*, 2008]. The optimum conditions for triggering a rising tone chorus element proposed by *Omura and Nunn* [2011] were also examined through comparison with the observed properties of the chorus emissions.

2. THEMIS Observation

[6] In the present study we use data from the THEMIS mission [*Angelopoulos*, 2008]; the Electric Field Instrument (EFI) [*Bonnell et al.*, 2008], the Search-Coil Magnetometer (SCM) [*Le Contel et al.*, 2008; *Roux et al.*, 2008], the Fluxgate Magnetometer (FGM) [*Auster et al.*, 2008], and the Electro-Static Analyzer (ESA) [*McFadden et al.*, 2008]. The EFI and SCM waveforms sampled at 8192 Hz were analyzed in this study. We first converted the waveform data of SCM and EFI into the magnetic field-aligned coordinates by referring to the FGM measurements to compute the wave normal angle and the Poynting vector of chorus emissions. The wave normal angle is computed by analyzing three components of the wave magnetic field using the method of *Samson and Olson* [1980], which has an inherent ambiguity of 180 degrees in the wave normal angle direction. Since the wave normal direction has a component in the direction of the energy flow, the ambiguity can be removed by introducing the Poynting vector **S**. The Poynting vector **S** in the frequency domain is calculated directly using $\mathbf{S}(f) = \mathrm{Re}\{\mathbf{E}(f) \times \mathbf{B}^*(f)\}/2\mu_0$, where $\mathbf{E}(f)$

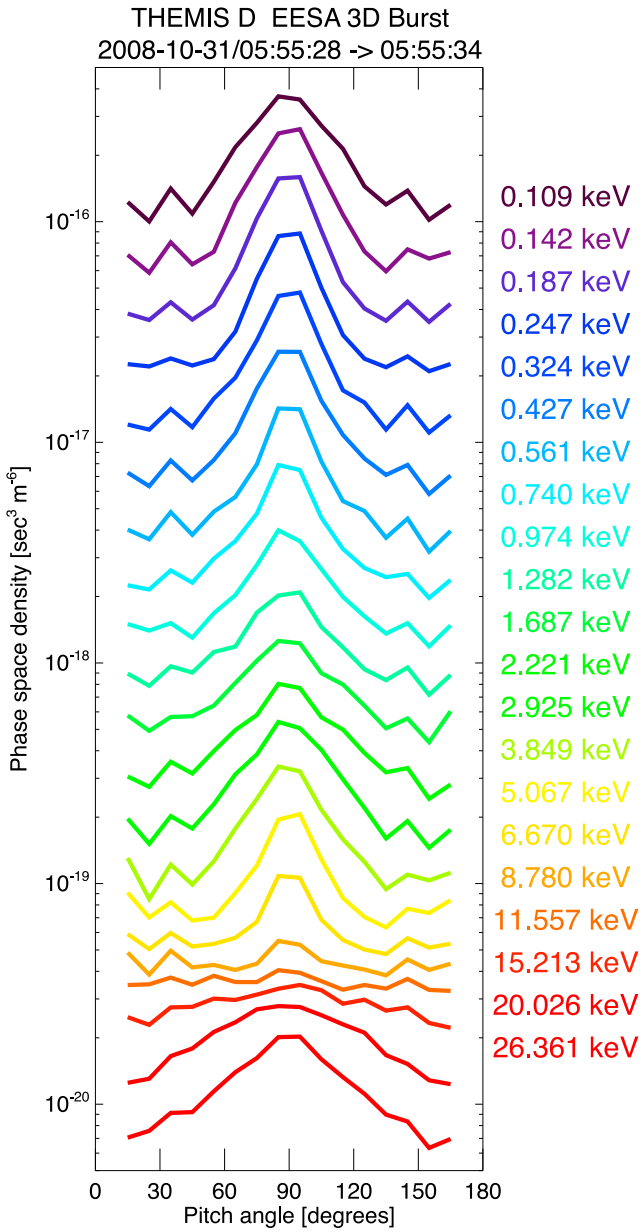

Figure 2. Electron pitch angle distribution observed by THEMIS D during the time interval shown in Figure 1.

and $\mathbf{B}(f)$ are the complex Fourier transformation of the electric and magnetic fields, μ_0 represents the magnetic permittivity in the vacuum, * indicates the complex conjugate, and Re stands for the real part.

[7] EFI measurements also provide individual sensor potentials, which are used to estimate spacecraft floating potential. Combining spacecraft floating potential with electron thermal speed measured by ESA, we can estimate total plasma density including cold plasma population that cannot be measured by ESA. Details are described in *Li et al.* [2010]. Total plasma density used in this study is evaluated from this method.

[8] Figure 1a shows the spectra of wave magnetic field component perpendicular to the ambient magnetic field direction observed by THEMIS D on 31 October 2008. During the observation, THEMIS D was located at a radial distance of 6.10 R_E, at a magnetic local time of 5.61 hours, and at a magnetic latitude of 2.54 degrees. The location of THEMIS D estimated from the T96 magnetic field [*Tsyganenko*, 1995, 1996] is ~700 km northward from the magnetic equator. In Figure 1a we find a band of weak whistler mode waves just below 1000 Hz and discrete chorus elements with rising tones in the frequency range from 1000 to 2500 Hz without a distinct gap of wave amplitude at half the gyrofrequency (1540 Hz, denoted by the dotted line).

[9] Figure 2 shows pitch angle distributions of energetic electrons measured during the event. We find anisotropic distributions in the energy range below and above ~10 keV, while ~10 keV electrons show isotropic distributions. From the cyclotron resonance condition, we evaluated that the minimum resonant energies of whistler mode waves in the frequency range from 0.3 to 0.5 Ω_e are in the range from 4 keV to 20 keV, while the minimum resonance energy of whistler mode waves around 1000 Hz is ~20 keV. In the computation of the resonance condition, we assumed the total plasma density of 1.7 cm^{-3} and the gyrofrequency of 3080 Hz based on the observation. These estimations suggest that the isotropic distributions of ~10 keV electrons are the result of the pitch angle scattering through the resonant interaction with the chorus emissions, while the anisotropic distributions in the energy range above 20 keV can be a signature of free energy sources of the whistler mode waves that trigger the rising tone chorus elements.

[10] In Figure 1b, we show the wave normal angle of components having the magnetic wave spectral intensity larger than 10^{-5} nT^2/Hz. In the present study, we focus on five chorus elements as labeled in Figure 1b. The chorus elements propagate typically in the field-aligned direction in the entire frequency range. In Figure 1c, the Poynting vector parallel to the ambient magnetic field is shown. It is found that the selected chorus elements propagate southward although THEMIS D was located in the northern hemisphere. Using the Cluster multispacecraft observations, *Santolík et al.* [2004] reported that the central position of the chorus source region flaps at timescales of minute within 1000–2000 km of the geomagnetic equator. Thus, the observed Poynting vector direction can be explained by the flapping motion of the central position of the chorus source region. This idea is validated by the observation by THEMIS D two minutes after the event in Figure 1, which is shown in Figure 3. The data shown in Figure 3 was obtained at a radial distance of 6.16 R_E, at a magnetic local time of 5.64 hours, and at a magnetic latitude of 2.53 degrees. During this time interval, chorus emissions similar to those in Figure 1 are observed and the Poynting vector direction of the chorus elements changes from northward to southward. It is strongly suggested that the central position of the chorus source region flapped and crossed the location of THEMIS D around the time interval. Based on the result of *Santolík et al.* [2004], the distance from the spacecraft location to the chorus source is small enough to assume the observation was made within the source region. Since the spacecraft position close to the central position of the chorus source, the propagation effects on the waves are not significant.

[11] The frequency profile, wave normal angle, and propagation direction of the chorus emissions are consistent with the properties of rising tone chorus elements near the source region expected from the nonlinear wave growth theory

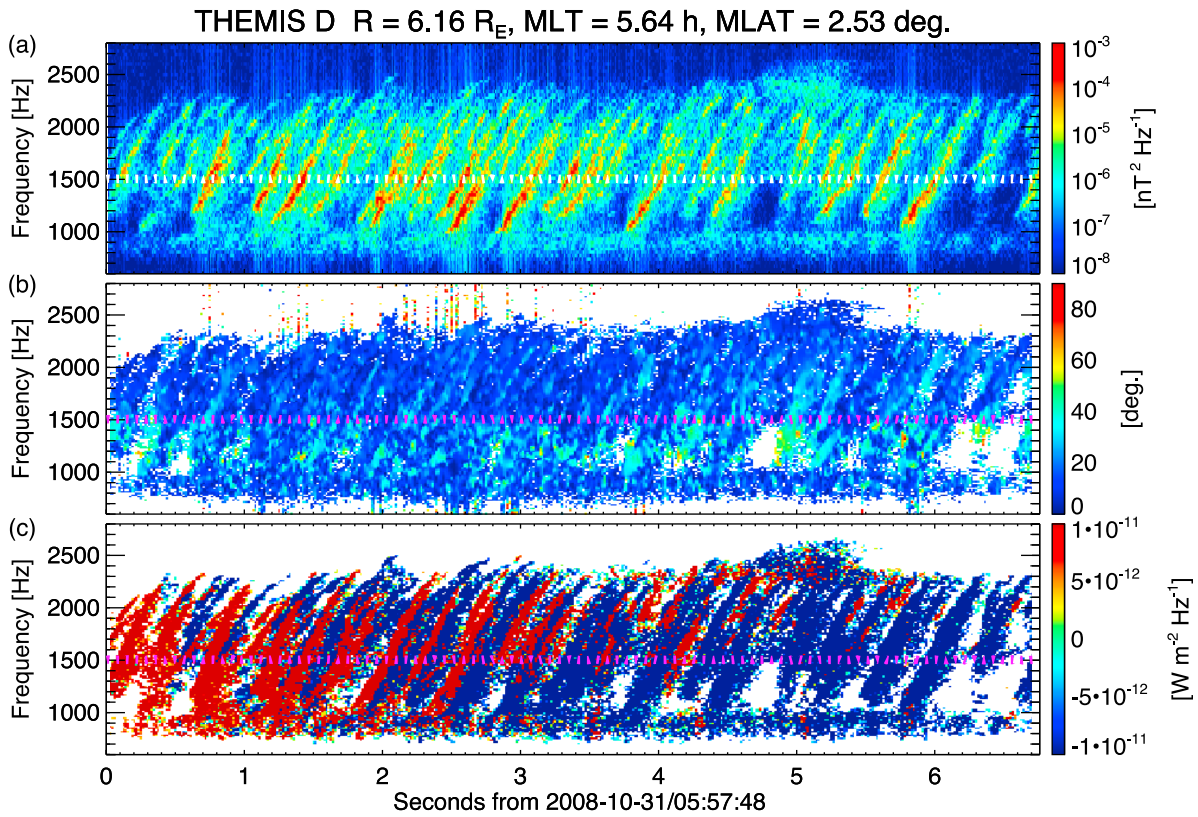

Figure 3. The same format as Figure 1 for an event observed from 05:57:48 to 05:57:54.8 UT on 31 October 2008 by THEMIS D. The results of Figures 3b and 3c are shown only when the magnetic wave spectral intensity is greater than 10^{-7} nT^2/Hz.

[*Omura et al.*, 2008, 2009]. The frequency sweep rates and the frequency profiles of the labeled chorus elements are studied in the next section. We do not analyze the properties of the chorus elements shown in Figure 3 because the overlap of the elements in time makes it difficult to pick up the properties of each individual chorus element.

3. Comparison With the Nonlinear Wave Growth Theory

3.1. Frequency Sweep Rates

[12] First, we study the frequency sweep rate of the observed chorus elements. Using the relativistic second-order resonance condition for a whistler mode wave with a varying frequency, *Omura et al.* [2008] showed that the sweep rate of the wave frequency ω is described as

$$\frac{\partial\omega}{\partial t} = \frac{0.4\chi}{\gamma\xi}\frac{V_{\perp 0}}{c}\frac{\omega}{\Omega_{e0}}\left(1-\frac{V_R}{V_g}\right)^{-2}\frac{B_W}{B_0}\Omega_{e0}^2, \qquad (1)$$

where $\chi^2 = \left(1+\xi^2\right)^{-1}$, $\xi^2 = \omega(\Omega_e-\omega)/\omega_{pe}^2$, ω_{pe} is the electron plasma frequency, $\gamma = \left[1-\left(v_\parallel^2+v_\perp^2\right)/c^2\right]^{-1/2}$, $v_\parallel$ and $v_\perp$ are parallel and perpendicular velocity components of an electron, c is the speed of light, $V_{\perp 0}$ is the average value of $v_\perp$ of energetic electrons, V_R is the resonance velocity, V_g is the group velocity, B_W is the amplitude of the wave magnetic field, and B_0 is the background magnetic field intensity. Equation (1) shows that the frequency sweep rate of a chorus element depends on the amplitude of the wave magnetic field near the magnetic equator. We estimated the frequency sweep rate by equation (1) and compared with the observation.

[13] For comparison of the theory and observation, we studied the instantaneous frequencies of chorus elements by using the zero crossings of one of the perpendicular components of the wave magnetic field. Figures 4a–4c show the time histories of the instantaneous frequencies of the elements 1, 3, and 5 shown in Figure 1b. The instantaneous frequencies of the chorus elements gradually increase in time. In each panel of Figure 4, we also show line segments with the tilt corresponding to the theoretically estimated frequency sweep rate by equation (1) at each time period (~0.16 s). In evaluating equation (1), we assumed the plasma density of 1.7 cm^{-3} and the typical kinetic energy of energetic electrons of 20 keV based on the spacecraft floating potential measurements and the ESA observations, respectively. The theoretically estimated frequency sweep rates are basically consistent with the observed frequency variations of elements 1 to 4 (elements 2 and 4 are not shown). In element 5, however, we find that the theoretical sweep rates tend to be larger than the observed sweep rates. According to the nonlinear wave growth theory, the frequency sweep rate of each chorus element is determined in the region close to the magnetic equator. In the region away from the source, the wave amplitude of a chorus element is nonlinearly intensified during its propagation. This effect would results in the deviation of the theoretically estimated

sweep rate from the observation. Since element 5 has the largest wave amplitude among the five elements, it is possible that element 5 is a chorus element generated relatively away from THEMIS D and it is nonlinearly amplified through its propagation, resulting in the deviation of the estimated sweep rate from the observation.

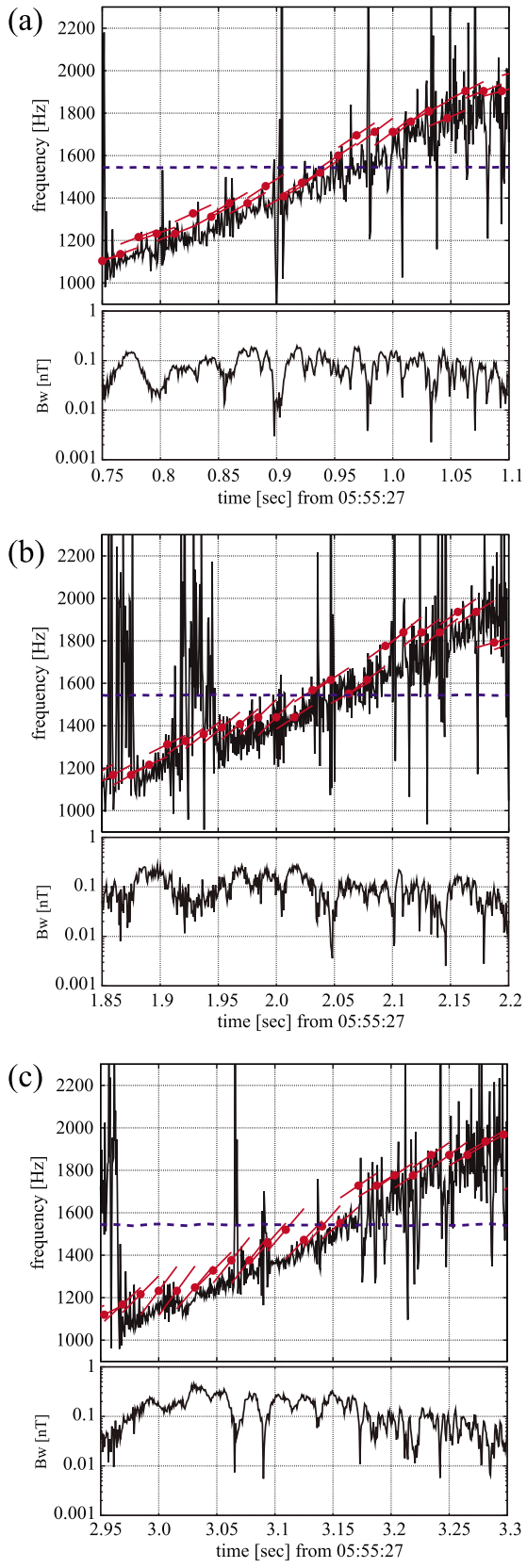

3.2. Threshold and Optimum Wave Amplitudes

[14] *Omura and Nunn* [2011] studied the optimum wave amplitudes for generation of a rising tone chorus element. The optimum wave amplitude Ω_{wo} is derived from the consideration of the nonlinear transition time T_N, corresponding to the timescale of the formation process of the electromagnetic electron hole. The optimum wave amplitude Ω_{wo} normalized by Ω_{e0}, $\tilde{\Omega}_{wo} = \Omega_{wo}/\Omega_{e0}$, is given by

$$\tilde{\Omega}_{wo} = 0.81\pi^{-5/2}\frac{Q}{\tau}\frac{s_1\tilde{V}_g}{s_0\tilde{\omega}\tilde{U}_{t\|}}\left(\frac{\tilde{\omega}_{ph}\tilde{V}_{\perp 0}\chi}{\gamma}\right)^2\exp\left(-\frac{\gamma^2\tilde{V}_R^2}{2\tilde{U}_{\|}^2}\right), \quad (2)$$

where Q represents the depth of the electromagnetic electron hole in the velocity phase space, τ is the ratio of T_N to the nonlinear trapping period $T_{tr} = 2\pi/\omega_{tr}$, ω_{tr} is the trapping frequency [*Omura et al.*, 2008], $s_0 = V_{\perp 0}\chi/\xi c$, $s_1 = \gamma\left(1 - V_R/V_g\right)^2$, $\tilde{V}_g = V_g/c$, $\tilde{\omega} = \omega/\Omega_{e0}$, $\tilde{U}_{t\|} = U_{t\|}/c = \gamma V_{t\|}/c$, $\tilde{\omega}_{ph} = \omega_{ph}/\Omega_{e0}$, $\omega_{ph} = \omega_{pe}(N_h/N_{e0})^{1/2}$, $\tilde{V}_{\perp 0} = V_{\perp 0}/c$, and $\tilde{V}_R = V_R/c$. $V_{t\|}$, N_h, and N_{e0} are thermal velocity of energetic electrons parallel to the ambient magnetic field, number density of hot and cold electrons, respectively. The optimum wave amplitude was compared with the simulation results and found that the τ = 0.25–1.0 shows good agreement between the theory and simulation [*Omura and Nunn*, 2011; *Hikishima and Omura*, 2012]. The threshold of the wave amplitude for the nonlinear wave growth of chorus emissions has been theoretically derived by *Omura et al.* [2009]. The equation of the threshold $B_{w,th}$ is given by $B_{w,th}/B_0 = \tilde{\Omega}_{th}$, where

$$\tilde{\Omega}_{th} = \frac{100\pi^3\gamma^3\xi}{\tilde{a}\tilde{\omega}\tilde{\omega}_{ph}^4\tilde{V}_{\perp 0}^5\chi^5}\left(\frac{\tilde{a}s_2\tilde{U}_{t\|}}{Q}\right)^2\exp\left(\frac{\gamma^2\tilde{V}_R^2}{\tilde{U}_{t\|}^2}\right), \quad (3)$$

$\tilde{a} = ac^2/\Omega_{e0}^2$, and a is specified by the L value and the Earth's radius R_E as $a = 4.5/(LR_E)^2$.

[15] In the generation mechanism of a rising tone chorus element, based on the nonlinear wave growth theory, a coherent wave element emerges from a band of incoherent whistler mode waves in the frequency range lower than the typical chorus emissions. Therefore we first examined equation (3) by assuming a range of parameters of energetic electrons referring to the initial wave amplitude of the observed chorus elements. Figure 5 shows the wave amplitudes of the chorus elements at

Figure 4. Instantaneous frequencies analyzed from the waveform data of one of the perpendicular components of the wave magnetic field of (a) element 1, (b) element 3, and (c) element 5. The theoretically estimated frequency sweep rates are shown in the top panels of Figures 4a–4c by the slopes of red line segments, while the center of each red line segment represents the frequency of the maximum wave amplitude at the corresponding time period of the spectra shown in Figure 1a. The dashed blue line in each panel shows half the local gyrofrequency. The bottom panels of Figures 4a–4c show the time history of the amplitude of the wave magnetic field perpendicular to the ambient magnetic field.

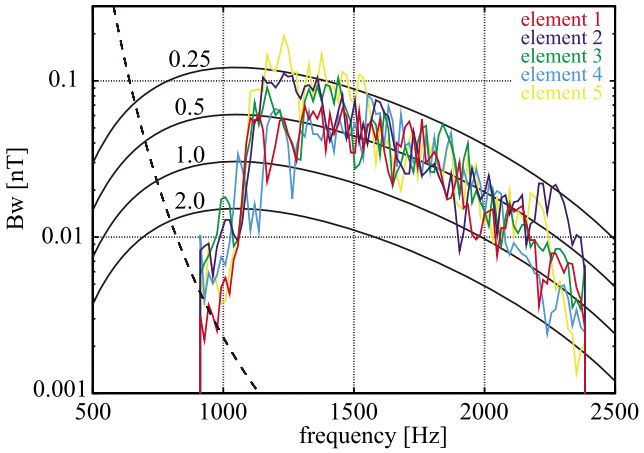

Figure 5. Frequency profiles of the wave amplitudes of the chorus elements. Solid lines show the optimum wave amplitudes with different values of τ denoted by the attached numbers, and the dashed line represents the threshold of the wave amplitude for the nonlinear wave growth.

different frequencies estimated from the local maximum values of the frequency spectra shown in Figure 1. The suitable threshold amplitude at 1000 Hz is obtained in a case that $N_h = 4 \times 10^{-3} N_{e0}$ and $T_\perp/T_\parallel = 1.5$, where $T_\perp$ and $T_\parallel$ are perpendicular and parallel temperatures of energetic electrons, respectively. In the calculation of the threshold wave amplitudes, the $Q = 0.5$ is assumed [*Omura and Nunn*, 2011]. The estimated threshold of the wave amplitude by equation (3) is shown in Figure 5. We then estimated the optimum wave amplitude by equation (2) using the same parameters of energetic electrons. The estimated optimum wave amplitudes for different values of τ are shown in Figure 5, and the frequency profile of Ω_{wo} with $\tau \sim 0.5$ is consistent with the frequency profiles of the observed chorus elements. The number density of energetic electrons assumed in the theoretical computation is roughly consistent with the energetic electron flux from ESA showing that the number density of energetic electrons (>20 keV) is 1.0×10^{-2} relative to the total number density of electrons. These results reveal that the generation process of the observed chorus elements are well explained by the nonlinear wave growth theory.

4. Summary

[16] We analyzed the waveform data obtained from THEMIS and reported the rising tone chorus elements without a gap at half the gyrofrequency in the region close to the magnetic equator. We studied the properties of the observed chorus elements and showed that the observed frequency sweep rates are consistent with the estimates based on the nonlinear wave growth theory. In addition, we compared the frequency profiles of the chorus wave amplitudes with those of the optimum and threshold wave amplitudes for generating rising tone chorus emissions derived from the nonlinear wave growth theory. The results of the comparison show the reasonable agreement between the observed properties of chorus elements and the theoretical estimates, indicating that the triggering process of rising tone emissions with the optimum amplitudes is continually taking place in the generation process of a rising tone chorus element.

[17] Although our results suggest that the upper-band chorus and lower-band chorus are originally a single emission due to the nonlinear wave growth mechanism, the generation process of upper-band and lower-band chorus is still an open issue. Further investigations are required to understand the generation mechanisms such as nonlinear wave damping due to oblique propagation [*Omura et al.*, 2009] and excitation in ducts of either enhanced or depleted cold plasma density [*Bell et al.*, 2009]. We have found other periods of the THEMIS observation showing chorus elements without a gap at 0.5 Ω_e in the region close to the magnetic equator. Detailed analyses on these events would yield important clues in understanding the generation mechanism of both upper-band and lower-band chorus emissions from the point of view of the nonlinear wave-particle interactions. We leave the analyses as a target of our future work.

[18] **Acknowledgments.** We would like to acknowledge NASA contract NAS5-02099 for use of data from the THEMIS Mission, J. Bonnell for use of EFI data, J. P. McFadden for use of ESA data, U. Auster for use of FGM data, and the German Ministry for Economy and Technology and the German Center for Aviation and Space (DLR) under contract 50 OC 0302. The French involvement (SCM instruments) on THEMIS are supported by CNES and CNRS-INSU. This work was supported by grant-in-aid 22684025, 23224011, 23340147 and the Global COE program "Global Education and Research Center for Earth and Planetary Dynamics" at Tohoku University of the Ministry of Education, Culture, Sports, Science and Technology in Japan. S. K. is supported by a research fellowship of the Japan Society for the Promotion of Science for Young Scientists.

[19] Robert Lysak thanks the reviewers for their assistance in evaluating the paper.

References

Angelopoulos, V. (2008), The THEMIS mission, *Space Sci. Rev.*, *141*(1–4), 5–34, doi:10.1007/s11214-008-9336-1.

Auster, H. U., et al. (2008), The THEMIS fluxgate magnetometer, *Space Sci. Rev.*, *141*(1–4), 235–264, doi:10.1007/s11214-008-9365-9.

Bell, T. F., U. S. Inan, N. Haque, and J. S. Pickett (2009), Source regions of banded chorus, *Geophys. Res. Lett.*, *36*, L11101, doi:10.1029/2009GL037629.

Bonnell, J. W., et al. (2008), The electric field instrument (EFI) for THEMIS, *Space Sci. Rev.*, *141*(1–4), 303–341, doi:10.1007/s11214-008-9469-2.

Burtis, W. J., and R. A. Helliwell (1976), Magnetospheric chorus: Occurrence patterns and normalized frequency, *Planet. Space Sci.*, *24*, 1007–1024.

Cully, C. M., V. Angelopoulos, U. Auster, J. Bonnell, and O. Le Contel (2011), Observational evidence of the generation mechanism for rising-tone chorus, *Geophys. Res. Lett.*, *38*, L01106, doi:10.1029/2010GL045793.

Hikishima, M., and Y. Omura (2012), Particle simulations of whistler-mode rising-tone emissions triggered by waves with different amplitudes, *J. Geophys. Res.*, *117*, A04226, doi:10.1029/2011JA017428.

Hikishima, M., S. Yagitani, Y. Omura, and I. Nagano (2009), Full particle simulation of whistler-mode rising chorus emissions in the magnetosphere, *J. Geophys. Res.*, *114*, A01203, doi:10.1029/2008JA013625.

Katoh, Y., and Y. Omura (2011), Amplitude dependence of frequency sweep rates of whistler mode chorus emissions, *J. Geophys. Res.*, *116*, A07201, doi:10.1029/2011JA016496.

Le Contel, O., et al. (2008), First results of the THEMIS searchcoil magnetometers, *Space Sci. Rev.*, *141*(1–4), 509–534, doi:10.1007/s11214-008-9371-y.

Li, W., R. M. Thorne, J. Bortnik, Y. Nishimura, V. Angelopoulos, L. Chen, J. P. McFadden, and J. W. Bonnell (2010), Global distributions of suprathermal electrons observed on THEMIS and potential mechanisms for access into the plasmasphere, *J. Geophys. Res.*, *115*, A00J10, doi:10.1029/2010JA015687.

Li, W., J. Bortnik, R. M. Thorne, and V. Angelopoulos (2011), Global distribution of wave amplitudes and wave normal angles of chorus waves using THEMIS wave observations, *J. Geophys. Res.*, *116*, A12205, doi:10.1029/2011JA017035.

Macúšová, E., et al. (2010), Observations of the relationship between frequency sweep rates of chorus wave packets and plasma density, *J. Geophys. Res.*, *115*, A12257, doi:10.1029/2010JA015468.

McFadden, J. P., C. W. Carlson, D. Larson, M. Ludlam, R. Abiad, B. Elliott, P. Turin, M. Marckwordt, and V. Angelopoulos (2008), The THEMIS ESA plasma instrument and in-flight calibration, *Space Sci. Rev.*, *141*(1–4), 277–302, doi:10.1107/s11214-008-9440-2.

Meredith, N. P., R. B. Horne, and R. R. Anderson (2001), Substorm dependence of chorus amplitudes: Implications for the acceleration of electrons to relativistic energies, *J. Geophys. Res.*, *106*, 13,165–13,178, doi:10.1029/2000JA900156.

Omura, Y., and D. Nunn (2011), Triggering process of whistler-mode chorus emissions in the magnetosphere, *J. Geophys. Res.*, *116*, A05205, doi:10.1029/2010JA016280.

Omura, Y., D. Nunn, H. Matsumoto, and M. J. Rycroft (1991), A review of observational, theoretical and numerical studies of VLF triggered emissions, *J. Atmos. Terr. Phys.*, *53*, 351–368.

Omura, Y., Y. Katoh, and D. Summers (2008), Theory and simulation of the generation of whistler-mode chorus, *J. Geophys. Res.*, *113*, A04223, doi:10.1029/2007JA012622.

Omura, Y., M. Hikishima, Y. Katoh, D. Summers, and S. Yagitani (2009), Nonlinear mechanisms of lower-band and upper-band VLF chorus emissions in the inner magnetosphere, *J. Geophys. Res.*, *114*, A07217, doi:10.1029/2009JA014206.

Roux, A., O. Le Contel, C. Coillot, A. Bouabdellah, B. de la Porte, D. Alison, S. Ruocco, and M. C. Vassal (2008), The search coil magnetometer for THEMIS, *Space Sci. Rev.*, *141*(1–4), 265–275, doi:10.1007/s11214-008-9455-8.

Samson, J. C., and J. V. Olson (1980), Some comments on the description of the polarization states of waves, *Geophys. J. R. Astron. Soc.*, *61*, 115–129.

Santolík, O., D. A. Gurnett, J. S. Pickett, M. Parrot, and N. Cornilleau-Wehrlin (2003), Spatio-temporal structure of storm-time chorus, *J. Geophys. Res.*, *108*(A7), 1278, doi:10.1029/2002JA009791.

Santolík, O., D. A. Gurnett, J. S. Pickett, M. Parrot, and N. Cornilleau-Wehrlin (2004), A microscopic and nanoscopic view of storm-time chorus on 31 March 2001, *Geophys. Res. Lett.*, *31*, L02801, doi:10.1029/2003GL018757.

Tao, X., W. Li, J. Bortnik, R. M. Thorne, and V. Angelopoulos (2012), Comparison between theory and observation of the frequency sweep rates of equatorial rising tone chorus, *Geophys. Res. Lett.*, *39*, L08106, doi:10.1029/2012GL051413.

Trakhtengerts, V. (1995), Magnetosphere cyclotron maser: Backward wave oscillator generation regime, *J. Geophys. Res.*, *100*, 17,205–17,210.

Trakhtengerts, V. Y., A. G. Demekhov, E. E. Titova, B. V. Kozelov, O. Santolik, D. Gurnett, and M. Parrot (2004), Interpretation of Cluster data on chorus emissions using the backward wave oscillator model, *Phys. Plasmas*, *11*, 1345–1351.

Tsurutani, B. T., and E. J. Smith (1974), Postmidnight chorus: A substorm phenomenon, *J. Geophys. Res.*, *79*, 118–127, doi:10.1029/JA079i001p00118.

Tsyganenko, N. A. (1995), Modeling the Earth's magnetospheric magnetic field confined within a realistic magnetopause, *J. Geophys. Res.*, *100*, 5599–5612.

Tsyganenko, N. A. (1996), Effects of the solar wind conditions on the global magnetospheric configuration as deduced from data-based field models, *Eur. Space Agency Spec. Publ.*, *ESA SP-389*, 181–185.